IN-34

175563

p. 20

A Rapid-Distortion-Theory Turbulence Model for Developed Unsteady Wall-Bounded Flow

G.J. Brereton
Insitute for Computational Mechanics in Propulsion
Lewis Research Center
Cleveland, Ohio

The University of Michigan
Ann Arbor, Michigan

and

R.R. Mankbadi
Lewis Research Center
Cleveland, Ohio

(NASA-TM-106249) A
RAPID-DISTORTION-THEORY TURBULENCE
MODEL FOR DEVELOPED UNSTEADY
WALL-BOUNDED FLOW   (NASA)   20 p

N93-32199

Unclas

G3/34   0175563

July 1993

NASA

A RAPID-DISTORTION-THEORY TURBULENCE MODEL FOR

DEVELOPED UNSTEADY WALL-BOUNDED FLOW

G.J. Brereton*
Institute for Computational Mechanics in Propulsion
Lewis Research Center
Cleveland, Ohio 44135

and

R.R. Mankbadi
National Aeronautics and Space Administration
Lewis Research Center
Cleveland, Ohio 44135

Abstract

A new approach to turbulence modeling in unsteady developed flows has recently been introduced [1], based on results of rapid distortion theory. The approach involves closing the κ-ℓ equations for the organized unsteady component of the flow by modeling local unsteadiness as a rapid distortion of the local structure of the parent turbulent flow, in terms of an effective strain parameter α_{eff} [2]. In this paper, the phase-conditioned equations of motion are developed to accomodate a new unsteady dissipation model and local effects of the slow-relaxation time scale of the parent flow. The model equations are tested against measurements of the response of a fully-developed turbulent pipe flow to the superposition of sinusoidal streamwise oscillation. Good agreement is found between measurements and predictions over a wide range of frequencies of unsteadiness, indicating that this approach may be particularly well suited to modeling of unsteady turbulent flows which are perturbations about a well characterized mean.

1. INTRODUCTION

Turbulent flows which feature organized unsteady bulk motion are present in numerous aerodynamic, engineering and biological devices. In recent years, these flows have received considerable attention within the canonical geometries of pipes, channels, and flat-plate boundary layers, under external forcings such as continuous sinusoidal streamwise ones which are well suited to analytical treatment. The boundary-layer studies of Karlsson [3], Cousteix *et al.* [4], and Brereton *et al.* [5], the channel-flow research of Tardu *et al.* [6], and the pipe-flow experiments of Tu & Ramaprian [7], Shemer *et al.* [8], Mao & Hanratty [9], and Hwang & Brereton [10] have a covered a wide range of the parameter space accessible to laboratory experiments. A general conclusion from these studies is that mean flow profiles of velocity and turbulent stresses are scarcely

---

*Department of Mechanical Engineering and Applied Mechanics,
The University of Michigan, Ann Arbor, Michigan 48109

distinguishable from counterparts measured in steady flow, with the same average external conditions. The average state of the flow is then practically independent of either the amplitude or frequency of forcing. This observation suggests modeling approaches which treat forced unsteady flows as perturbations about a parent mean flow, the structure of which may be deduced from the large body of information on steady turbulent wall-bounded flows.

Modeling of unsteady turbulent flows has typically been pursued by solving unsteady evolution equations incorporating closures based on steady flow information. Examples include the Reynolds stress and κ-ϵ calculations of Kebede et al. [11], low-Reynolds number κ-ϵ modeling of Cotton & Ismael [12], quasi-steady κ-ϵ computations of Mankbadi & Mobark [13], κ-ω models of Wilcox [14], and the multi-scale models of Wilcox [15] and Kim & Chen [16], applied to unsteady flows in [17]. These approaches are problematic when near-wall and low Reynolds number functions are employed in steady flow forms, since the steady flow relations between near-wall turbulent measures and the momentary value of u_τ no longer apply because of variation in phase of velocities with distance from the wall. While attempts have been made to calculate unsteady flows using near-wall functions based on a momentary local turbulent Reynolds number, these approaches to modeling remain under development.

Modeling efforts which decouple the mean and unsteady components of the velocity field include some preliminary channel-flow models proposed by Acharya & Reynolds [18] (quasi-steady perturbations on the mean flow, one-equation κ closure) and the recent model of Mankbadi & Liu [1], based on results of rapid distortion theory applied to homogeneous turbulent flow. In the latter model, a κ-ϵ formulation of the oscillatory component of the velocity field was closed by modeling the momentary structure of the perturbation field (in this case, the local ratio of oscillatory Reynolds stress to oscillatory turbulent kinetic energy) as a function of the effective strain α_{eff} in the perturbed flow. The excellent qualitative (though not quantitative) agreement of predicted turbulent kinetic energy profiles with measured data prompted a closer examination of this model. The results of a revised rapid distortion turbulence model and comparisons with new, high-frequency oscillatory pipe-flow data are described in this paper.

2. EXPERIMENTS

Profiles of streamwise velocity and turbulent intensity in fully-developed oscillatory pipe flow were measured in a recirculating water facility with a translucent test section (57mm in diameter, 160 diameters long, assuring fully-developed flow at downstream locations). Flow control was achieved by motoring a profiled sleeve around a longitudinal slot milled in the pipe near its downstream end, under the control of a laboratory computer. The mean flow Reynolds number (referenced to centerline velocity and pipe diameter) was 11,700, with a burst frequency of about 1.7 Hz. Forced oscillation at up to 10 Hz could be achieved in this apparatus, with temporal variation of phase-averaged velocity always a good representation of a sine wave. In these experiments the amplitude

of oscillation at the pipe centerline varied between 19% of the mean centerline velocity at 0.25 Hz and 11% at 4.0 Hz. Further details are provided in Hwang & Brereton [10].

Measurements of streamwise velocity were made using a laser-Doppler anemometer with frequency shifting and a counter, which was interfaced with a laboratory computer to allow phase-resolved measurements of the instantaneous velocity of the flow. Since highly repeatable periodic motion could be imposed by the flow-control apparatus, a phase-averaging procedure was adopted for decomposition of flow variables into mean, oscillatory and turbulent components. Statistical convergence in data was assumed to have been reached when the fractional tolerance (a measure of differences in $\langle u'u' \rangle$ over the first and second halves of the data set, normalized by the rms level in $\langle u'u' \rangle$) reached 0.1%, which typically required at least 1000 ensembles. Here $\langle \ \rangle$ denotes the phase average of the argument.

3. PHASE-CONDITIONED $K - \ell$ EQUATIONS

In close proximity to the pipe wall, the radial wall-normal distance $R - r$ may be replaced by y and a cartesian representation used. The triple decomposition and appropriate time and phase averaging operations allow any general dependent variable, $f(\mathbf{x}, t)$, to be expressed as the summed contribution of the three parts:

$$f(\mathbf{x}, t) = \overline{f}(\mathbf{x}) + \widetilde{f}(\mathbf{x}, t) + f'(\mathbf{x}, t) , \tag{1}$$

which are the mean or time-averaged one, the oscillatory or periodic one, and the turbulent component respectively. For fully developed swirl-free flow, the constant-property Navier-Stokes equations may be decomposed to yield a streamwise oscillatory momentum equation:

$$\frac{\partial \widetilde{u}}{\partial t} = -\frac{1}{\rho} \frac{\partial \widetilde{p}}{\partial x} - \frac{\partial}{\partial y} \widetilde{u'v'} + \nu \frac{\partial^2 \widetilde{u}}{\partial y^2} \tag{2}$$

and an oscillatory turbulent kinetic energy equation:

$$\frac{\partial \widetilde{\kappa}}{\partial t} = -\widetilde{u'v'} \frac{\partial \widetilde{u}}{\partial y} - \widetilde{u'v'} \frac{\partial U}{\partial y} - \widetilde{u'v'} \frac{\partial \widetilde{u}}{\partial y} - \frac{\partial}{\partial y} \left(\frac{1}{\rho} \widetilde{v'p'} + \widetilde{v'\kappa} - \nu \frac{\partial \widetilde{\kappa}}{\partial y} \right) - \widetilde{\epsilon} \tag{3}$$

where both $\frown$ and $\sim$ are oscillatory operators and $\widetilde{\epsilon}$ is the oscillatory component of the homogeneous dissipation rate. If oscillatory diffusion is assumed to be dominated by viscous effects near the wall, rather than turbulent transport or pressure work, and second-harmonic turbulence production is a negligible proportion of the fundamental, the $\widetilde{\kappa}$ equation may be simplified as:

$$\frac{\partial \widetilde{\kappa}}{\partial t} = -\widetilde{u'v'} \frac{\partial \widetilde{u}}{\partial y} - \widetilde{u'v'} \frac{\partial U}{\partial y} + \nu \frac{\partial^2 \widetilde{\kappa}}{\partial y^2} - \widetilde{\epsilon} . \tag{4}$$

3

While $\frac{\partial U}{\partial y}$ and $-\overline{u'v'}$ may be taken from benchmark data on the steady parent flow [17, 18, 26], a $\widetilde{\kappa} \sim \widetilde{u'v'}$ closure must be devised to be consistent with results of rapid distortion theory, together with an $\widetilde{\epsilon}$ model equation which is physically plausible and of the correct asymptotic near-wall form.

4. RAPID DISTORTION THEORY CLOSURE

Although rapid distortion theory was originally proposed to estimate how turbulence is distorted during rapid passage through large-scale straining motions [19], more recent studies have shown that this linear theory retains a high level of applicability to slowly changing turbulent shear flows [20] — nonlinear processes tend to limit the development which would take place under rapid distortion rather than alter the structure of turbulence. In this spirit, Maxey [2] demonstrated how *steady* turbulent flows in pipes and channels with local values of the structural parameter $-\overline{u'v'}/\overline{u'u'}$ could be interpreted as locally-uniform shear flows which rapidly distorted turbulence of an initially axisymmetric spectrum tensor at the necessary local strain to produce the same turbulence structure. Thus results of rapid distortion theory could be used to ascribe local values of an effective rapid-distortion strain α_{eff} to steady wall-bounded turbulent shear flows; structural parameters such as $-\overline{u'v'}/\overline{u'u'}$ and $-\overline{u'v'}/\kappa$ could then be expressed as functions of α_{eff}.

The asymptotic strain relations of:

$$\frac{\partial \alpha}{\partial t} = \frac{\partial U}{\partial y} , \tag{5}$$

from the definition of strain through rapid distortion at short timescales, and:

$$\alpha = T \frac{\partial U}{\partial y} \tag{6}$$

which recovers the limit of equilibrium flow with T as a local slow-distortion (large eddy) timescale, suggest the generalized local relation which satisfies the asymptotic strains:

$$\frac{\partial \alpha}{\partial t} = \frac{\partial U}{\partial y} - \frac{\alpha}{T} , \tag{7}$$

which may also be presumed to model the effective strain α_{eff} in perturbations about a steady flow [2]. For the case of streamwise oscillations upon a fully developed parent flow, the dominant components of the perturbation and mean shear strains are the same. It therefore appears attractive to model the former in terms of the latter.

The $\widetilde{\kappa} \sim \widetilde{u'v'}$ closure is formed by first expressing $-\overline{u'v'}/\overline{\kappa} = F(\alpha_{\text{eff}})$, where $F(\alpha_{\text{eff}})$ is evaluated directly from experimental data (*i.e.* Laufer [21], Lawn [22]). For oscillations

4

which result in small perturbations of α_{eff} about its local parent-flow value, with $\alpha_{\text{eff}} = \overline{\alpha}_{\text{eff}} + \widetilde{\alpha}_{\text{eff}}$, $F(\alpha_{\text{eff}})$ may be linearized as:

$$F(\alpha_{\text{eff}}) = F(\overline{\alpha}_{\text{eff}}) + \widetilde{\alpha}_{\text{eff}} F'(\overline{\alpha}_{\text{eff}}) \tag{8}$$

leading to the linearized $\widetilde{\kappa} \sim \widetilde{u'v'}$ and $\widetilde{\alpha}_{\text{eff}}$ relations:

$$-\widetilde{u'v'} = F(\overline{\alpha}_{\text{eff}}) \widetilde{\kappa} + \widetilde{\alpha}_{\text{eff}} F'(\overline{\alpha}_{\text{eff}}) \overline{\kappa} \quad \text{and} \quad \frac{\partial \widetilde{\alpha}_{\text{eff}}}{\partial t} = \frac{\partial \widetilde{u}}{\partial y} - \frac{\widetilde{\alpha}_{\text{eff}}}{T} . \tag{9 a, b}$$

Rapid distortion theory characterizations may also be used to express components of the turbulent kinetic energy in terms of κ and a local effective strain. If $-\overline{u'v'}/\overline{u'u'} = G(\alpha_{\text{eff}})$, then small perturbation analysis leads to a relation for the oscillatory component of streamwise turbulence intensity in the form:

$$-\widetilde{u'v'} = G(\overline{\alpha}_{\text{eff}}) \widetilde{u'u'} + \widetilde{\alpha}_{\text{eff}} G'(\overline{\alpha}_{\text{eff}}) \overline{u'u'} \tag{10}$$

enabling $\widetilde{u'u'}$ to be evaluated from F, G, and $-\overline{u'v'}$ from the parent flow, after computation of $\widetilde{\kappa}$. Typical characterizations of $G(\alpha_{\text{eff}})$ in fully developed turbulent pipe flow are shown in Fig. 1 (from [2]).

The oscillatory rate of dissipation $\widetilde{\epsilon}$ is modeled in the form:

$$\widetilde{\epsilon} = \text{const.} \, \widetilde{\kappa} \frac{\sqrt{\overline{\kappa}}}{\overline{\ell}} \tag{11}$$

where $\overline{\ell}$ is a local length scale of dissipation of the parent flow. Thus the phase-averaged rate of dissipation $\langle \epsilon \rangle$ is the phase-conditioned turbulent kinetic energy $\langle \kappa \rangle$ divided by the local small-eddy time scale $\overline{\ell}/\sqrt{\overline{\kappa}}$. In essence, $\langle \epsilon \rangle$ is treated as proportional to the time-dependent turbulent kinetic energy $\langle \kappa \rangle$ supplied to the small scales, dissipated over time scales of the parent flow; $\widetilde{\epsilon}$ is then the unsteady part of $\langle \epsilon \rangle$. The assumption that the relevant dissipation time scales are those of the parent flow is justified if small scale effects are locally isotropic and out of tune with relatively low wavenumber organized forcing. The excellent agreement between high-frequency regions of energy spectra in forced and unforced boundary layers [23, 24] supports this view.

The correct *quasi-steady* near-wall behavior for the $\widetilde{\epsilon}$ model may be incorporated by an additive term which revises the time scale according to the proposal of Reynolds [25]. If the dissipation time scale $\overline{\ell}$ is taken as constant multiple of the local mixing length $\ell_m^2 = -\overline{u'v'}/(\partial U/\partial y)^2$, then the correct near-wall behavior in $\langle \epsilon \rangle$ may be achieved by setting

$$\widetilde{\epsilon} = c_1 \widetilde{\kappa} \frac{\sqrt{\overline{\kappa}}}{\overline{\ell}} \left(1 + \frac{c_2 \overline{\kappa}^{3/2}}{\overline{\ell}^3 (\partial U/\partial y)^3} \right) = c_1 \widetilde{\kappa} \frac{\sqrt{\overline{\kappa}}}{\overline{\ell}} \left(1 + c_2 \left(\frac{\overline{\kappa}}{-\overline{u'v'}} \right)^{3/2} \right) . \tag{12}$$

This approach simplifies the closure as a one-equation κ-ℓ closure in which the distribution of the dissipation length scale is taken directly from the mean flow. The model follows the asymptote of $\widetilde{\epsilon} = 0$ at high frequencies ($\langle \kappa \rangle$ frozen at its mean value of

$\overline{\kappa}$), with insufficient time for vortex stretching to reduce the scale of motions to the dissipation range and retain phase memory. It also matches the phase of $\widetilde{\epsilon}$ (plus oscillatory turbulent diffusion and pressure work) to the phase of $\widetilde{\kappa}$ — a more questionable assumption which can be assessed when full simulation data for unsteady flows become available.

The model constants scale the dissipation length scale $\overline{\ell}$ of the parent flow and may be deduced from near-wall steady flow-data.

$$\text{As} \quad y \to 0 , \quad \langle \epsilon \rangle = c_1 c_2 \langle \kappa \rangle^3 \frac{\partial \langle U \rangle}{\partial y} / \langle -u'v' \rangle^2 . \tag{13}$$

From the parent flow, or equivalently the steady channel-flow simulations of Kim et al. [26], $c_1 c_2 = 1.4 \times 10^{-4}$. The constant c_1 is evaluated from the local ratios of turbulence production to dissipation and $-\overline{u'v'}/\overline{\kappa}$ in the parent flow, at the point closest to the wall at which the near-wall correction to the dissipation length scale becomes negligible. From simulations of steady turbulent channel-flow [26], this correction reaches 4% at $y^+ \simeq 12$ where the ratio of turbulence production to dissipation is 1.3 and $-\overline{u'v'}/\overline{\kappa} = 0.15$. Setting the ratio of production to dissipation equal to $c_1 (\overline{\kappa}/ - \overline{u'v'})^{3/2}/$ yields $c_1 \simeq 0.08$, with comparable values of c_1 found at adjacent locations. In combination with the constraint on the size of the corrective term, c_1 should be evaluated as close to the wall as possible; dissipation is strongest in the wall region and is best modeled on parent flow data from that region. Also, if the assumption that dissipation takes place over a mean-flow time scale is not fully justified, this approach may also be interpreted as a quasi-steady model for dissipation, dominated by fine scale motions in the immediate vicinity of the wall, which adjust so rapidly to low wavenumber forcing that they effectively retain their steady equilibrium values (referenced to the wall variable $\overline{u}_\tau$). Away from the wall this is not the case; hence the desirability of a near-wall calibration of model coefficients.

5. SOLUTION PROCEDURE

The solution procedure required evaluation of $F(\overline{\alpha}_{\text{eff}})$, $\overline{\alpha}_{\text{eff}}$, $-\overline{u'v'}$, and $\frac{\partial U}{\partial y}$ at discrete y positions from benchmark data describing the parent flow. A local effective slow-distortion timescale $T(y)$ could then be deduced from (6) for each y value. A linear algebraic model of α_{eff} as a function of y^+, combined with the explicit $\partial u^+/\partial y^+$ model of Liakopoulos [27], led to a smoothly varying model for $T(y^+)$, plotted in Fig. 2. The model reproduces physically plausible features such as a reduced response time as the wall is approached and a necessary reduction in the average local size of large eddies.

By expressing the pressure in (2) as the inviscid core pressure, the closed equation set may be expressed as:

$$\frac{\partial \widetilde{u}}{\partial t} = \frac{\partial \widetilde{u}_\infty}{\partial t} - \frac{\partial}{\partial y}\widetilde{u'v'} + \nu \frac{\partial^2 \widetilde{u}}{\partial y^2} ; \qquad \frac{\partial \widetilde{\kappa}}{\partial t} = -\overline{u'v'}\frac{\partial \widetilde{u}}{\partial y} - \widetilde{u'v'}\frac{\partial U}{\partial y} + \nu \frac{\partial^2 \widetilde{\kappa}}{\partial y^2} - \widetilde{\epsilon} ;$$

6

$$-\widetilde{u'v'} = F(\overline{\alpha}_{\text{eff}})\,\widetilde{\kappa} - \frac{F'(\overline{\alpha}_{\text{eff}})}{F(\overline{\alpha}_{\text{eff}})}\,\overline{u'v'}\,\widetilde{\alpha}_{\text{eff}} \; ; \qquad \frac{\partial \widetilde{\alpha}_{\text{eff}}}{\partial t} = \frac{\partial \widetilde{u}}{\partial y} - \frac{\widetilde{\alpha}_{\text{eff}}}{T} \; ;$$

$$\widetilde{\epsilon} = c_1\,\widetilde{\kappa}\,\frac{\sqrt{\overline{\kappa}}}{\ell_m}\left(1 + c_2\left(\frac{\overline{\kappa}}{-\overline{u'v'}}\right)^{3/2}\right) \; ; \qquad \ell_m^2 = -\overline{u'v'}/(\partial U/\partial y)^2 \; . \qquad (14)$$

In order to separate variables, $\widetilde{u}$, $\widetilde{u'v'}$, $\widetilde{\kappa}$, and $\widetilde{\alpha}_{\text{eff}}$ were expressed as $\widehat{u}\,e^{i\omega t}$, $\widehat{u'v'}\,e^{i\omega t}$, $\widehat{\kappa}\,e^{i\omega t}$ and $\widehat{\alpha}_{\text{eff}}\,e^{i\omega t}$ (where $\widehat{\ }$ denotes a complex first-harmonic amplitude). The closed equation set (12) was then combined as a system of first-order ordinary differential equations for the pairs of amplitudes of the first harmonic components of $\widetilde{u}$, $\frac{\partial \widetilde{u}}{\partial y}$, $\widetilde{\kappa}$, and $\frac{\partial \widetilde{\kappa}}{\partial y}$ which were in phase and 90° out of phase with the far-field forcing (see Mankbadi & Liu [1] for details).

The structural coupling of the perturbed flow to the parent wall-bounded flow suggested normalization in wall units (referenced to $\overline{u}_\tau$ of the parent flow), which led to expressing frequency in the dimensionless form: $\omega^+ = \omega\nu/\overline{u}_\tau^2$. It has physical significance as the ratio of the near-wall viscous timescale of the parent flow to the timescale of forced unsteadiness. The equation system could be solved as a two point boundary value problem with $\widetilde{u}$ and $\widetilde{\kappa}$ equal to zero at the wall and with gradients of zero far from the wall, using a relaxation procedure with iteration by Newton's method. Integration was from the wall outward and required very high precision within the Stokes layer ($y \lesssim \sqrt{\nu/\omega}$) to preserve accuracy in the full-field solution. Norris & Reynolds [25] observed the same sensitivity in their steady $\kappa - \ell$ computations.

6. EXPERIMENTAL AND COMPUTATIONAL RESULTS

Experimental and computational results were compared in the near-wall region of turbulent pipe flow for values of ω^+ ranging from 0.01 to 0.16. The lower value corresponded to slow oscillation at which a quasi-steady response is approached, with small variations in the phase of measured quantities in the wall-normal direction. The upper value described a rapidly oscillating flow, at which the phase and amplitude of $\widetilde{u}$ were in good agreement with a (quasi-laminar) Stokes solution. Comparisons of the measured and computed amplitudes of $\widetilde{u}$, the amplitude of the oscillatory streamwise velocity, are shown in Fig. 3. While the high-frequency results are well matched by computations, which describe the characteristic overshoot in $\widetilde{u}$ quite well, discrepancies between model and experimental results grow with increasing wall-normal distance and decreasing frequency. The complementary model and experimental results for the phase of $\widetilde{u}$ (plotted as the phase advance relative to the phase of the centerline oscillatory velocity) are shown in Fig. 4. These results also exhibit discrepancies at low frequencies, which become more severe as the wall is approached

The amplitudes and phases of $\widehat{u'u'}$ obtained from this model are shown in Figs. 5 and 6. The shapes of the $|\widehat{u'u'}|$ profiles are in good agreement with measurements, though

7

they appear to slightly underestimate the data at high frequencies. Since the effect of imperfect phase-averaging (cycle-to-cycle variation) and wall vibration would be to increase the apparent measured amplitude, and since these experimental difficulties are more likely to be encountered at higher oscillation frequencies, they may explain some of the observed discrepancies. The shortcoming of the model in predicting $|\widehat{u'u'}|$ at $\omega^+ = 0.01$ for $y^+ > 20$ is probably due to the absence of an oscillatory turbulent diffusion term, which would be of importance for an adequate description of slowly changing $\widetilde{\kappa}$ away from the wall. Another possibility is that the assumptions of small distortions about a mean no longer apply when the amplitude of $\widehat{u}$ reaches 19% of the mean. The model's shortcomings at low frequencies might also account for the discrepancies in prediction of the phase and amplitude of $\widehat{u}$ for $\omega^+ = 0.01$ in Figs. 3 and 4.

The phase of $\widehat{u'u'}$ indicates good agreement between the model and data for $y^+ \gtrsim 10$, though the same caveats about predictions of the $\omega^+ = 0.01$ data apply. Closer to the wall, where the amplitude of $\widehat{u'u'}$ was underpredicted at high frequencies, discrepancies in phase become significantly larger. It is possible that smoothed near-wall ℓ model might produce better results, but at the cost of greater empiricism. In this region at high frequencies of unsteadiness, the treatment of turbulence as if in a locally uniform, rapidly distorted shear flow may be too simplistic in the immediate vicinity of the wall. A careful re-evaluation of $F(\alpha_{\text{eff}})$, $G(\alpha_{\text{eff}})$ and T in this region might then be required to improve model performance.

The use of a local large-eddy relaxation time scale $T(y)$, in preference to using the wall value throughout the flow, made little difference to predicted behavior. This observation reinforces the sensitivity of one-equation models to correct near-wall modeling, consistent with the observation for steady one-equation models that there is a narrow window for assumed values of ϵ_0 for which computations remain stable and can match external conditions.

While data describing other phase-conditioned measurements of the Reynolds-stress tensor are scarce, the dependence of wall shear stress $\langle \tau_0 \rangle$ on ω^+ has been measured by a number of researchers [7, 9, 10, 29]. The collapse of the phase of $\widehat{\tau}_0$ against ω^+ is well-established and serves as a good prediction test for turbulence models. The predicted phase dependence of $\widehat{\tau}_0$ is plotted in Fig. 7 against data reported from a number of different experiments and it is clear that the agreement is reasonable over all but the low frequencies for which experimental data are available. The asymptotic high-frequency approach to the 45° lead demanded by the Stokes solution is satisfied, and the transition region between $\omega^+ \simeq 0.008$ and $\omega^+ \simeq 0.03$ is predicted quite well, though the model shows a brief overshoot beyond 45° before reaching the high ω^+ asymptote. It is not clear if this represents a plausible physical effect masked by scatter in the data or if it is a shortcoming of the localized model, which an additional diffusion term in (7) might improve. The dimensionless form of the wall shear amplitude $\widehat{\tau}_0$ is plotted as a function of ω^+ in Fig. 8 and again shows reasonable qualitative agreement, though the overprediction of the model is pronounced. It is possible that the shortcomings

of a localized uniform-shear closure applied close to a solid surface contribute to this discrepancy in amplitude, though curiously not in phase.

In summarizing the model's performance, it can reproduce a large number of features of experimental data without any tuning to the unsteady flow, and exceeds appreciably the capabilities of quasi-steady models. There are clearly areas in which improvements can be made, and opportunities for more extensive testing against more detailed data sets. It seems likely that the absence of a momentary turbulence diffusion model, the simplicity of the strain evolution equation (7), and lack of distinction between wall-bounded and free uniform shear in rapid-distortion models, probably limit performance and should be areas for future refinement.

7. CONCLUSIONS

The modeling of unsteady turbulent flows as rapid distortions of a well-characterized parent mean flow represents a new and promising means of predicting turbulence in unsteady shear layers. This approach has been incorporated within a preliminary set of model equations for the oscillatory field for a wall-bounded unsteady turbulent flow which yields results in surprisingly good agreement with experimental data. The only empirical constants required for the model are obtained directly from the parent flow and so require no tuning. Some shortcomings of the model predictions indicate that opportunities for improved performance lie in: i) modeling of α_{eff} near boundaries; ii) development of α_{eff} evolution equations which match intermediate as well as asymptotic states; and iii) incorporation of non-linear α_{eff} structural models for flows with more extensive distortion about their mean. Also, several component equations of this model are proposed to match correct asymptotic forms, without specific regard to their intermediate behavior, and might benefit from smoothing through the addition of diffusion terms.

This modeling approach may also be applicable to non-equilibrium turbulent shear flows in which added distortion is principally in a direction other than that of the principal shear of the parent flow. In that case, development of more sophisticated rapid-distortion structural models might be pursued to build general turbulence models for various distortions about initial flow conditions.

8. ACKNOWLEDGEMENTS

9. REFERENCES

1   R. R. Mankbadi and J. T. C. Liu, *J. Fluid Mech.*, **238**, 55, (1992).

2   M. R. Maxey, *J. Fluid Mech.*, **124**, 261, (1982).

3   S. K. F. Karlsson, *J. Fluid Mech.*, **5**, 622, (1959).

4   J. Cousteix, R. Houdeville and J. Javelle, In *Unsteady Turbulent Shear Flows, IUTAM Symp.* (ed. R. Michel, J. Cousteix and R. Houdeville), 120, (1981).

5   G. J. Brereton, W. C. Reynolds and R. Jayaraman, *J. Fluid Mech.*, **221**, 131, (1990).

6   S. Tardu, G. Binder and R. Blackwelder, In *Advances in Turbulence*, (ed. G. Compte-Bellot and J. Mathieu), Springer-Verlag, (1987).

7   S. W. Tu and B. R. Ramaprian, *J. Fluid Mech.*, **137**, 31, (1983).

8   L. Shemer, I. Wygnanski and E. Kit, *J. Fluid Mech.*, 149, 313, (1984).

9   Z.-H. Mao and T. J. Hanratty, *J. Fluid Mech.*, **170**, 545, (1986).

10   J.-L. Hwang and G. J. Brereton, In *Turbulent Shear Flows 8*, (ed. B. L. Launder, U. Schumann and F. Durst), Springer-Verlag, (1992).

11   W. Kebede, B. E. Launder and B. A. Younis, *Proc. Fifth Symp. Turbulent Shear Flows*, Cornell University, (1985).

12   M. A. Cotton and J. O. Ismael, *Proc. Eighth Symp. Turbulent Shear Flows*, Munich, (1991).

13   R. R. Mankbadi and A. Mobark, *Journal of Heat and Fluid Flow*, **12**, 122, (1991).

14   D. C. Wilcox, *AIAA J.*, **26**, 11, 1299, (1988).

15   D. C. Wilcox, *AIAA J.*, **26**, 11, 1311, (1988).

16   S.-W. Kim and C. -P. Chen, *Numerical Heat Transfer*, 16, 2, 193, (1989).

17   S.-W. Kim, *NASA Contractors Rpt. 189176*, (1992).

18   M. Acharya and W. C. Reynolds, *Report TF-18*, Dept. of Mechanical Engineering, Stanford University, CA, (1975).

19   G. K. Batchelor and I. Proudman, *Q. J. Mech. Appl. Maths*, **7**, 83, (1954).

20   M. J. Lee, J. Kim and P. Moin, *J. Fluid Mech.*, **216**, 561, (1990).

21   J. Laufer, *NACA Rep. No. 1175*, (1954).

22   C. J. Lawn, *J. Fluid Mech.*, **48**, 477, (1971).

23   G. J. Brereton and W. C. Reynolds, *Phys. Fluids A*, **3** (1), 178, (1991).

24   J.-L. Hwang, Ph. D. Thesis, The University of Michigan, Ann Arbor, (1992).

25   W. C. Reynolds, *Annu. Rev. Fluid Mech.*, **8**, 183, (1976)

26   J. Kim, P. Moin and R. Moser, *J. Fluid Mech.*, **177**, 133, (1987).

27   A. Liakopoulos, *AIAA J.*, **22**, (6), 844 (1984).

28   L. H. Norris and W. C. Reynolds, *Eng. Rep FM-10*, Dept. of Mech. Eng., Stanford Univ. (1975)

29   D. S. Finnicum and T. J. Hanratty, *Proc. Sixth Symp. Turbulent Shear Flows*, Toulouse, (1987).
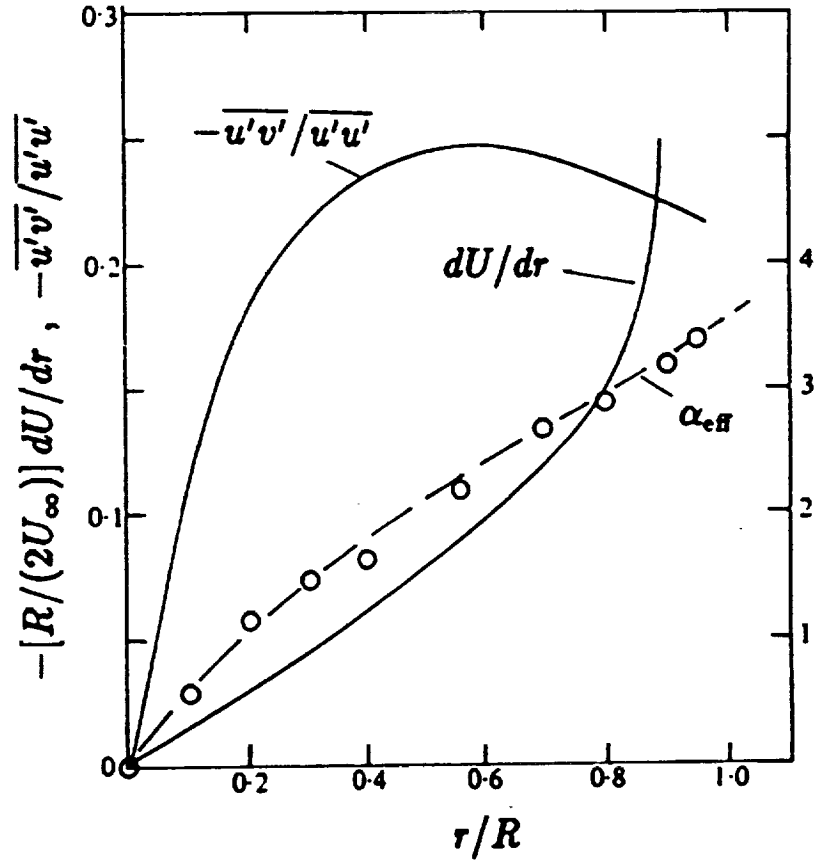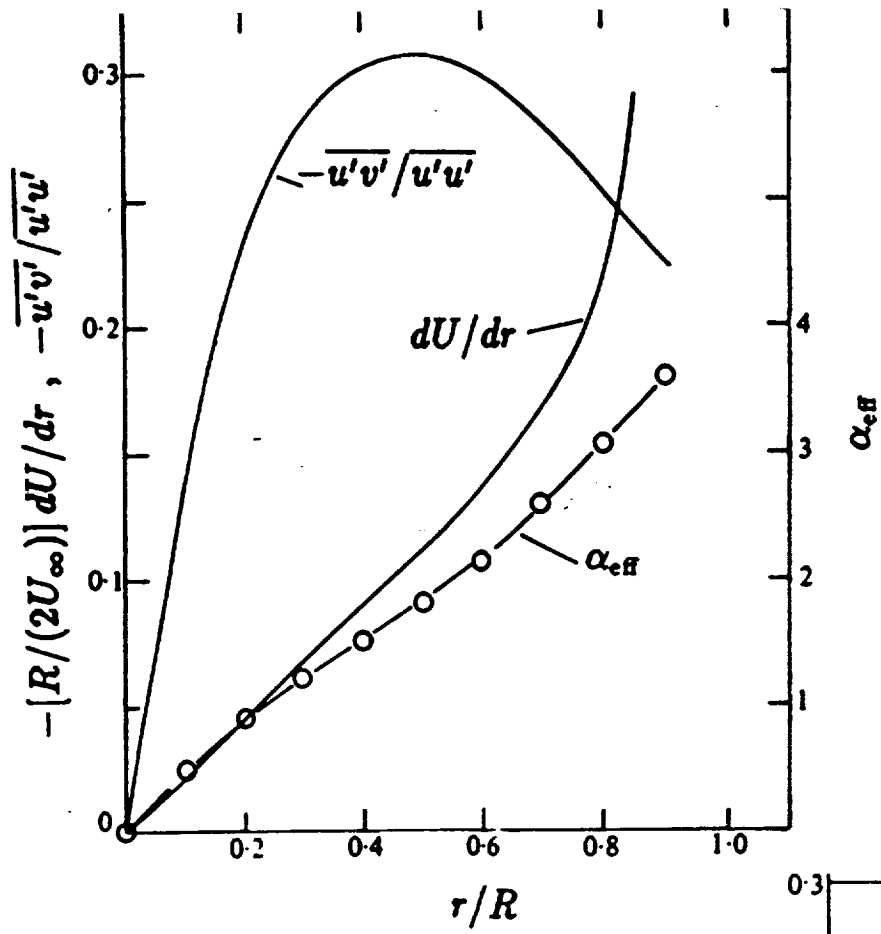
Fig. 1. Turbulent structural parameter $-\overline{u'v'}/\overline{u'u'}$ as a function of effective rapid-distortion strain, for fully developed pipe flow (Data from [21] left and [22] right).
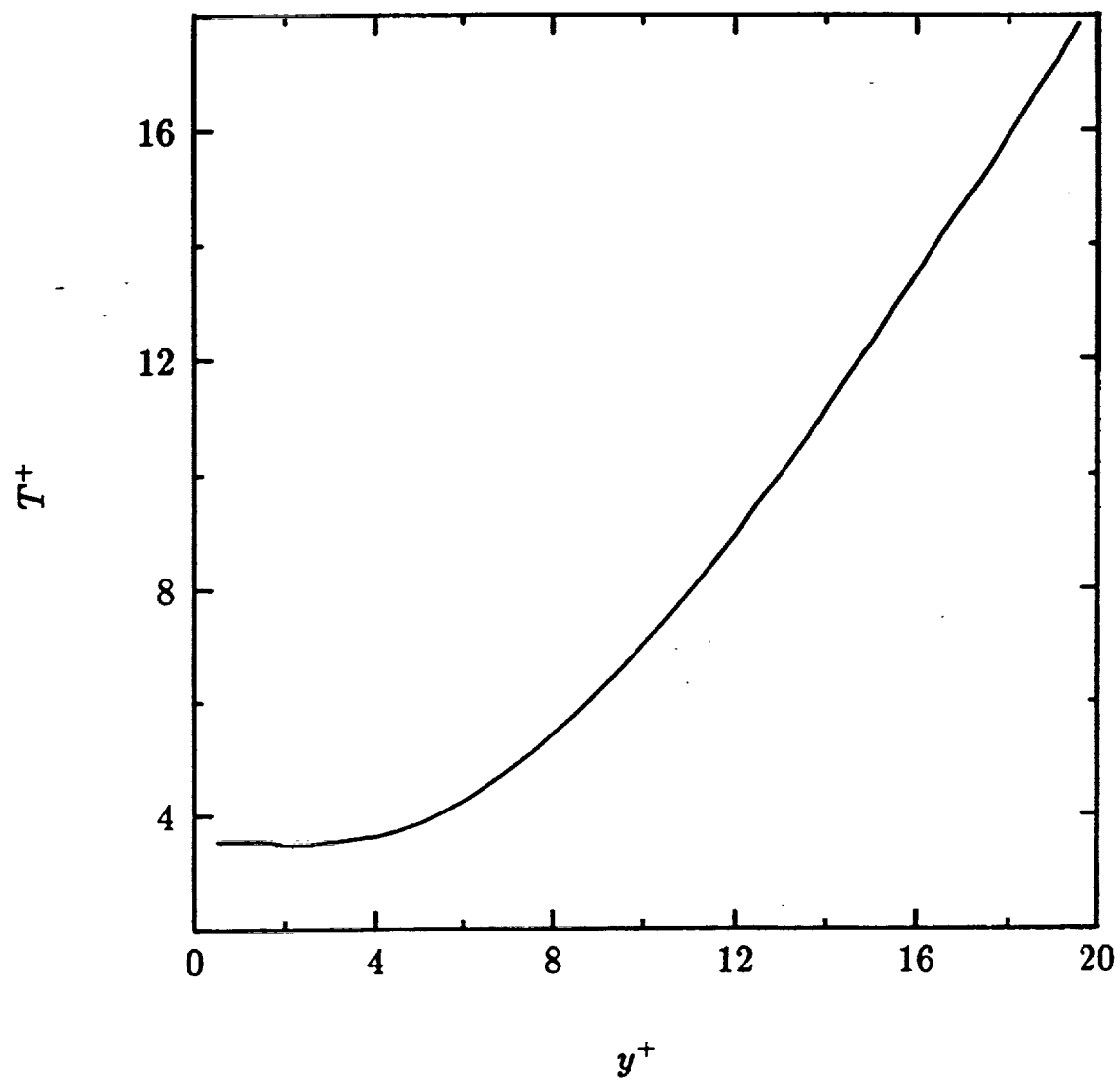
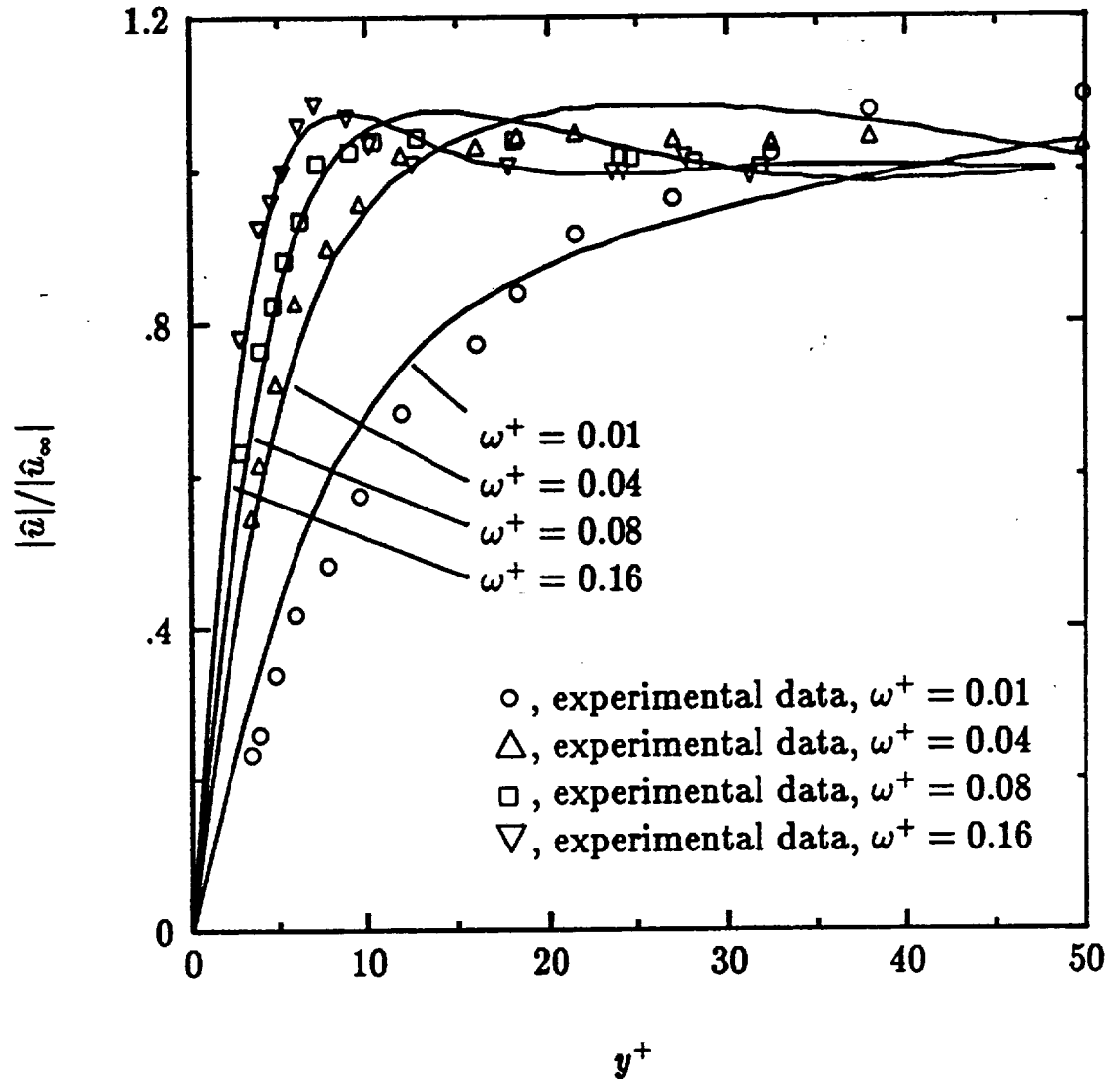**Fig. 2.** Large eddy relaxation time scale T^+ as a function of y^+.

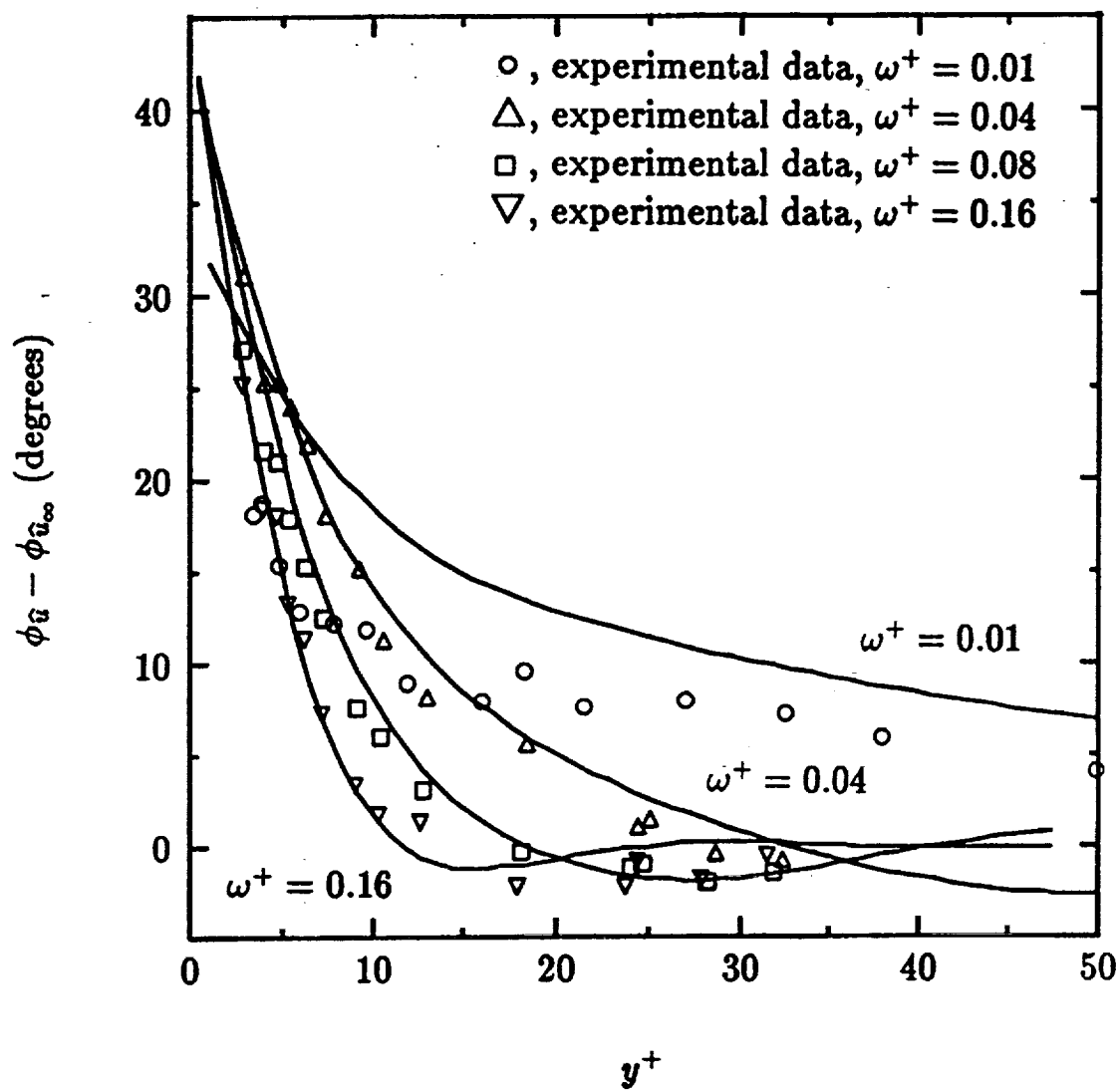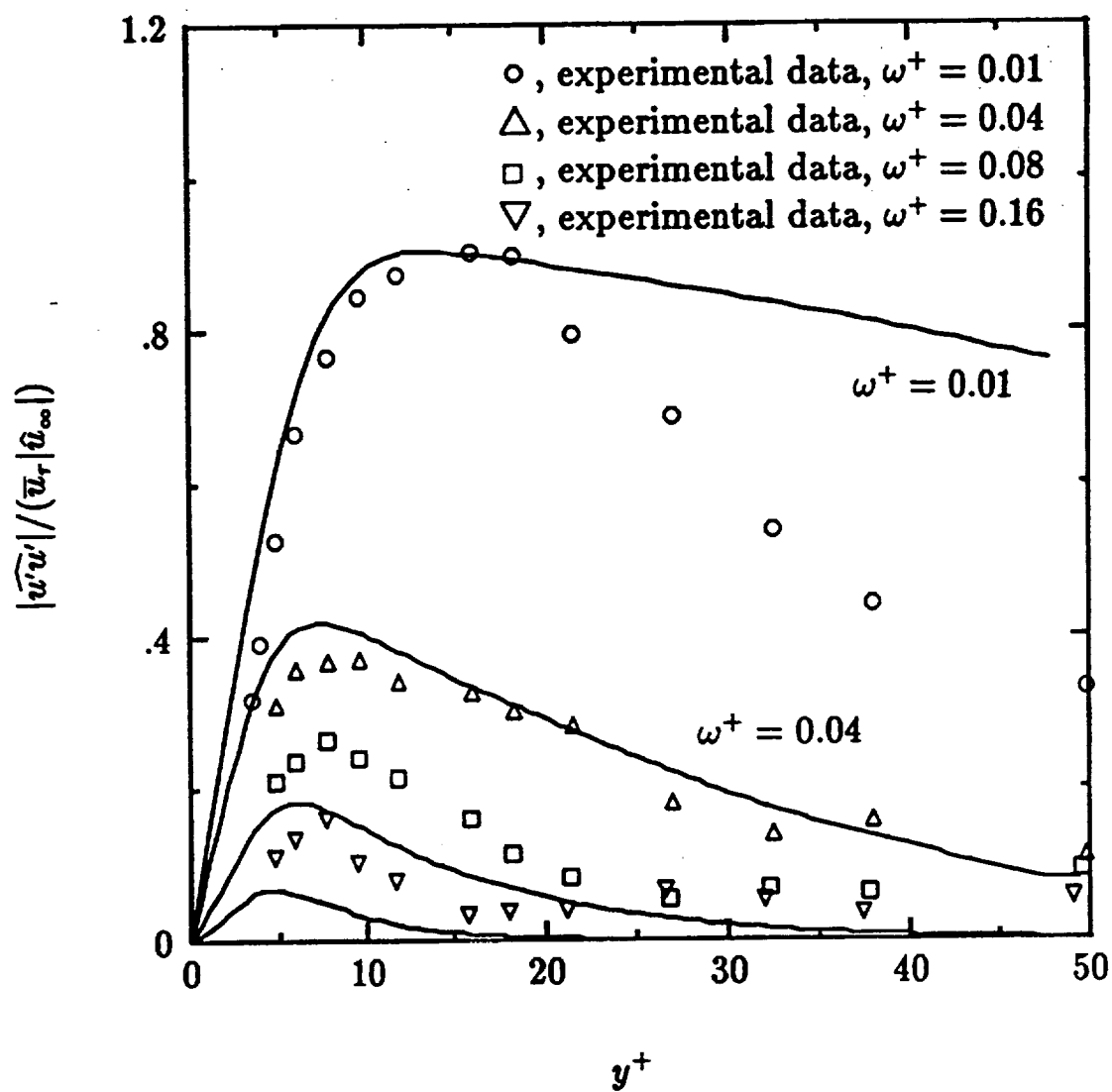Fig. 3. Measurements and predictions of $|\hat{u}|/|\hat{u}_\infty|$ as a function of y^+.

13

Fig. 4. Measurements and predictions of $(\phi_{\hat{u}} - \phi_{\hat{u}_\infty})$ as a function of y^+.

14

Fig. 5. Measurements and predictions of $|\widehat{u'u'}|/(\overline{u}_\tau|\widehat{u}_\infty|)$ as a function of y^+.
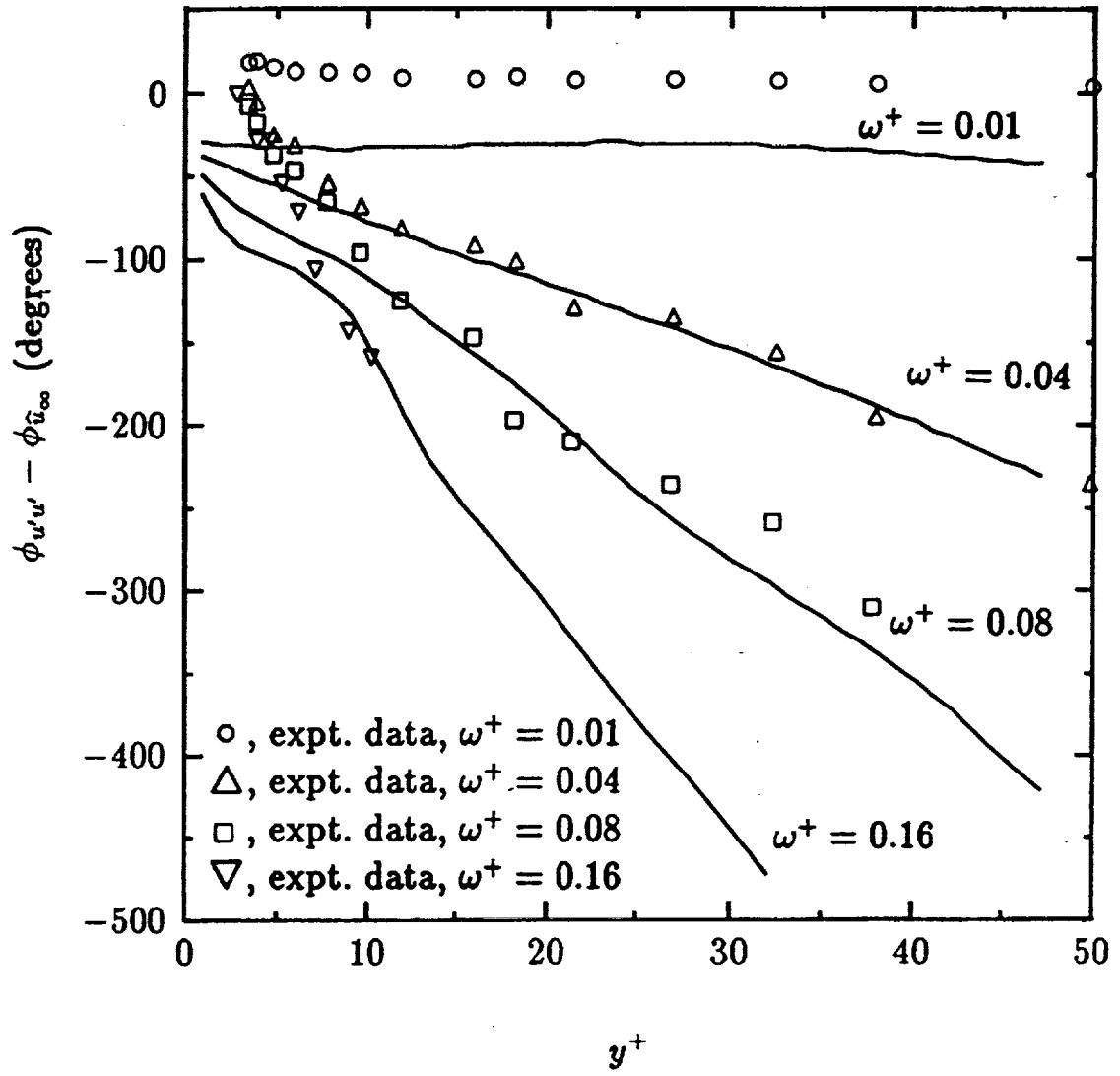
Fig. 6. Measurements and predictions of $(\phi_{\widehat{u'u'}} - \phi_{\widehat{u_\infty}})$ as a function of y^+.
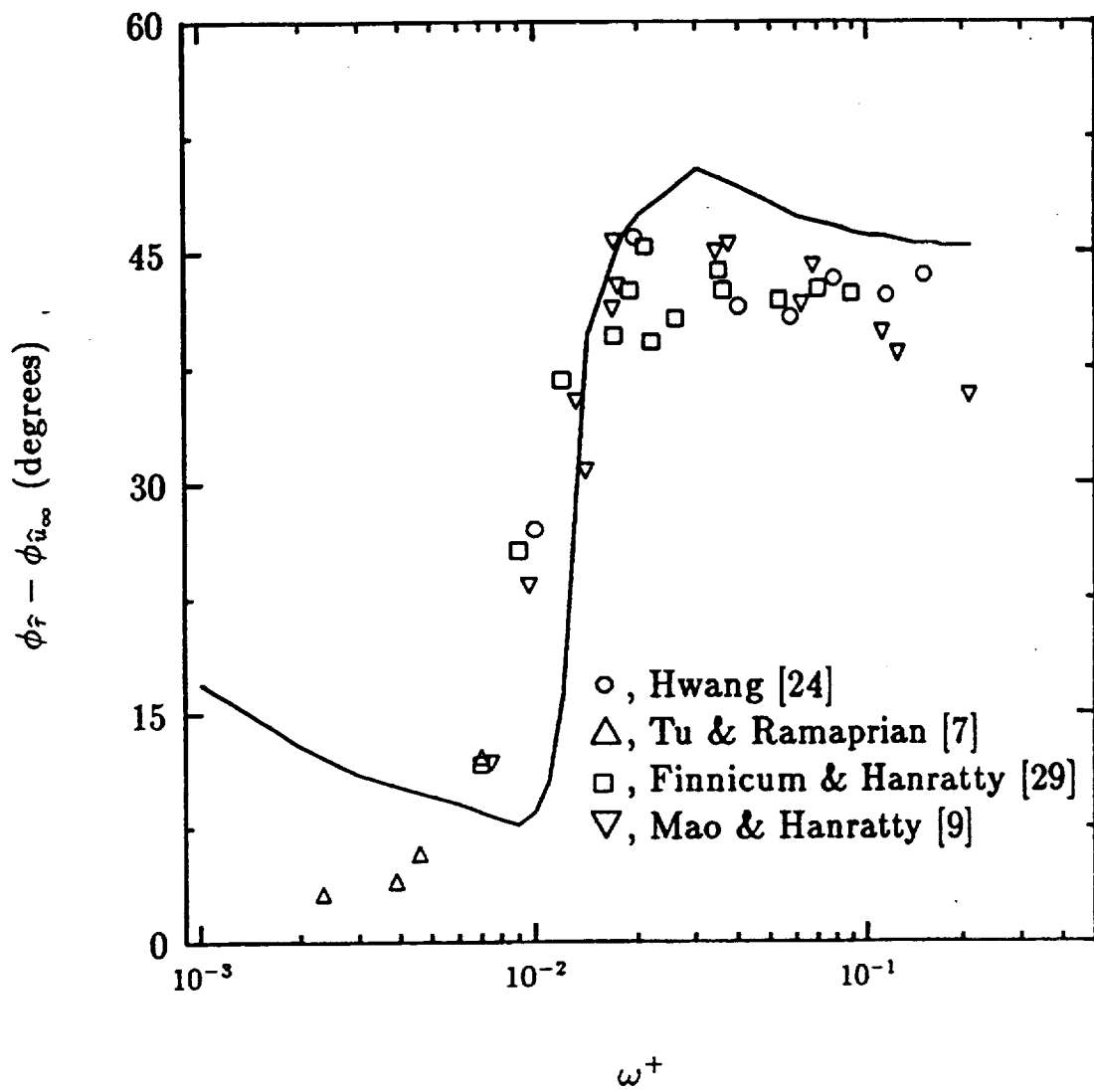
Fig. 7. Measured and predicted variation of $(\phi_{\widehat{\tau}_0} - \phi_{\widehat{u}_\infty})$ with ω^+.

17
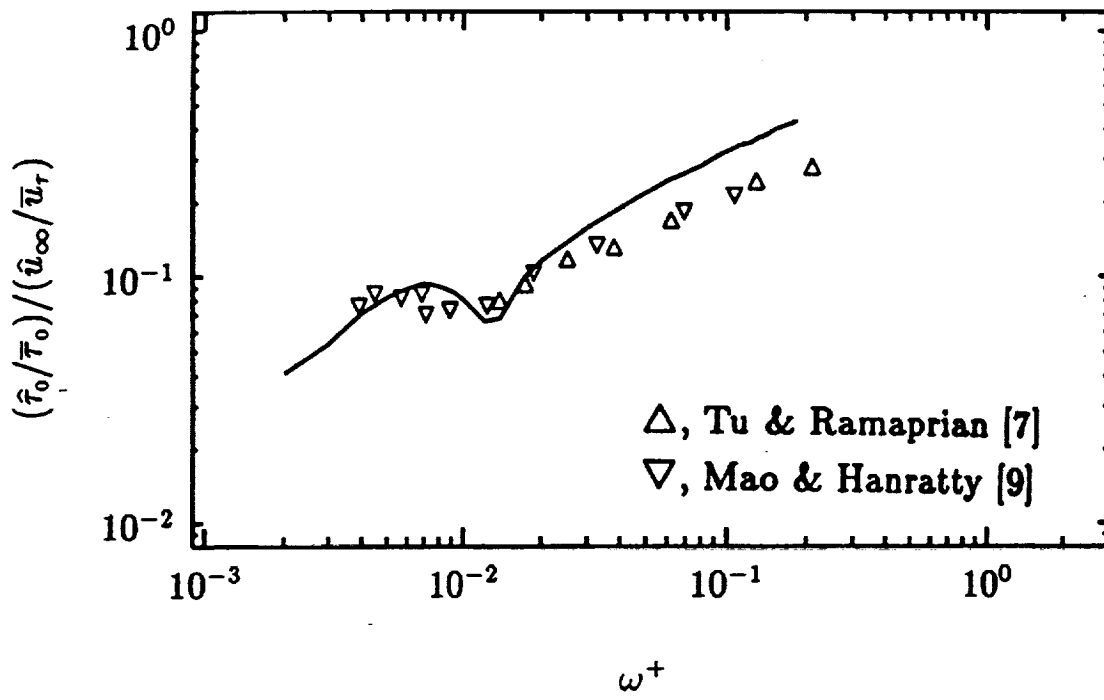
Fig. 8. Measured and predicted variation of $(\hat{\tau}_0/\bar{\tau}_0)/(\hat{u}_\infty/\bar{u}_\tau)$ with ω^+.

REPORT DOCUMENTATION PAGE

1. AGENCY USE ONLY (Leave blank)	2. REPORT DATE	3. REPORT TYPE AND DATES COVERED
	July 1993	Technical Memorandum

4. TITLE AND SUBTITLE

A Rapid-Distortion-Theory Turbulence Model for Developed Unsteady Wall-Bounded Flow

5. FUNDING NUMBERS

WU-505-90-5K

6. AUTHOR(S)

G.J. Brereton and R.R. Mankbadi

7. PERFORMING ORGANIZATION NAME(S) AND ADDRESS(ES)

National Aeronautics and Space Administration
Lewis Research Center
Cleveland, Ohio 44135-3191

8. PERFORMING ORGANIZATION REPORT NUMBER

E-7971

9. SPONSORING/MONITORING AGENCY NAME(S) AND ADDRESS(ES)

National Aeronautics and Space Administration
Washington, D.C. 20546-0001

10. SPONSORING/MONITORING AGENCY REPORT NUMBER

NASA TM-106249
ICOMP-93-22

11. SUPPLEMENTARY NOTES

12a. DISTRIBUTION/AVAILABILITY STATEMENT

Unclassified - Unlimited
Subject Category 34

12b. DISTRIBUTION CODE

13. ABSTRACT (Maximum 200 words)

A new approach to turbulence modeling in unsteady developed flows has recently been introduced [1], based on results of rapid distortion theory. The approach involves closing the κ-ℓ equations for the organized unsteady component of the flow by modeling local unsteadiness as a rapid distortion of the local structure of the parent turbulent flow, in terms of an effective strain parameter α_{eff} [2]. In this paper, the phase-conditioned equations of motion are developed to accommodate a new unsteady dissipation model and local effects of the slow-relaxation time scale of the parent flow. The model equations are tested against measurements of the response of a fully-developed turbulent pipe flow to the superposition of sinusoidal streamwise oscillation. Good agreement is found between measurements and predictions over a wide range of frequencies of unsteadiness, indicating that this approach may be particularly well suited to modeling of unsteady turbulent flows which are perturbations about a well characterized mean.

14. SUBJECT TERMS

Turbulence theory; Boundary layer; Unsteady flows; Rapid distortion theory

15. NUMBER OF PAGES

20

16. PRICE CODE

A03

17. SECURITY CLASSIFICATION OF REPORT	18. SECURITY CLASSIFICATION OF THIS PAGE	19. SECURITY CLASSIFICATION OF ABSTRACT	20. LIMITATION OF ABSTRACT
Unclassified	Unclassified	Unclassified	